AIP | Journal of Applied Physics

Piezoresponse force microscopy investigations of Aurivillius phase thin films

Lynette Keeney, Panfeng F. Zhang, Claudia Groh, Martyn E. Pemble, and Roger W. Whatmore

Citation: Journal of Applied Physics **108**, 042004 (2010); doi: 10.1063/1.3474959
View online: http://dx.doi.org/10.1063/1.3474959
View Table of Contents: http://scitation.aip.org/content/aip/journal/jap/108/4?ver=pdfcov
Published by the AIP Publishing

Piezoresponse force microscopy investigations of Aurivillius phase thin films

Lynette Keeney,[1,a)] Panfeng F. Zhang,[1] Claudia Groh,[2] Martyn E. Pemble,[1] and Roger W. Whatmore[1]
[1]*Tyndall National Institute, Lee Maltings, Cork, Ireland*
[2]*Department of Materials Science, Friedrich Schiller University of Jena, Germany*

(Received 7 October 2009; accepted 18 March 2010; published online 31 August 2010)

The sol-gel synthesis and characterization of $n \geq 3$ Aurivillius phase thin films deposited on $Pt/Ti/SiO_2-Si$ substrates is described. The number of perovskite layers, n, was increased by inserting $BiFeO_3$ into three layered Aurivillius phase $Bi_4Ti_3O_{12}$ to form compounds such as $Bi_5FeTi_3O_{15}$ ($n=4$). 30% of the Fe^{3+} ions in $Bi_5FeTi_3O_{15}$ were substituted with Mn^{3+} ions to form the structure $Bi_5Ti_3Fe_{0.7}Mn_{0.3}O_{15}$. The electromechanical responses of the materials were investigated using piezoresponse force microscopy and the results are discussed in relation to the crystallinity of the films as measured by x-ray diffraction. © *2010 American Institute of Physics*. [doi:10.1063/1.3474959]

I. INTRODUCTION

Single-phase multiferroics with ferroelectrically and magnetically combined structure at the atomic scale potentially allow for the tuning of the magnetoelectric effect in the quantum level as well as further control by the application of magnetic and/or electric fields. Such materials would offer a large application potential for functional devices that are able to convert signals from magnetic to electric and vice versa. The synthesis of new candidate multiferroics is driven by one of the biggest challenges facing the field of multiferroics today, namely, the need for room temperature multiferroic functionality.[1]

The Aurivillius[2] bismuth-based compounds represent an important class of piezoelectric compounds having the potential to present both ferroelectric and magnetoelectric transitions at the same time in a single phase.[3] The materials are members of an homologous series of Bi-layered oxides, consisting of $(Bi_2O_2)^{2+}$ layers alternating with $nABO_3$ perovskite units, described by the general formula $Bi_2O_2(A_{n-1}B_nO_{3n+1})$. These bismuth layer-structured ferroelectric materials have received increasing interest as lead free piezoelectric materials[4] with high Curie temperature (generally over 500 °C), fatigue-free switching characteristics making them suitable for nonvolatile memories[5] and a coupling between out of plane and in-plane polarization components making them interesting for electro-optic devices such as light valves.[6] On increasing the number of perovskite layers (n), the microstructural, magnetic, and physical properties of the materials can be altered significantly.[7–15]

Chemical doping of perovskite type materials, without producing a large decrease in their Curie temperature (T_c), has been useful in enhancing their electrical and magnetic properties.[9,16–20] Mn^{3+} doping has been reported to be effective for suppressing leakage current and improving the polarization switching properties of $Bi_4Ti_3O_{12}$ single crystals.[19] Other workers[9,21] have found that electrical conductivity in $Bi_5Ti_3Fe_{1-x}Mn_xO_{15}$ ($x=0-1$) ceramics increases with x. The Curie temperature was shifted toward the low temperature region at $x \geq 0.4$. Based on the idea that magnetoelectric coupling could be amplified near a transition temperature[22,23] and that ferromagnetic interactions should appear between the vacant Mn^{3+} *eg* orbital and the filled Fe^{3+} *eg* orbital in a perovskite structure,[24] Yang *et al.*[20] attempted to bring the Néel temperature of polycrystalline $BiFeO_3$ down to near room temperature (and thereby maximize the magnetoelec-

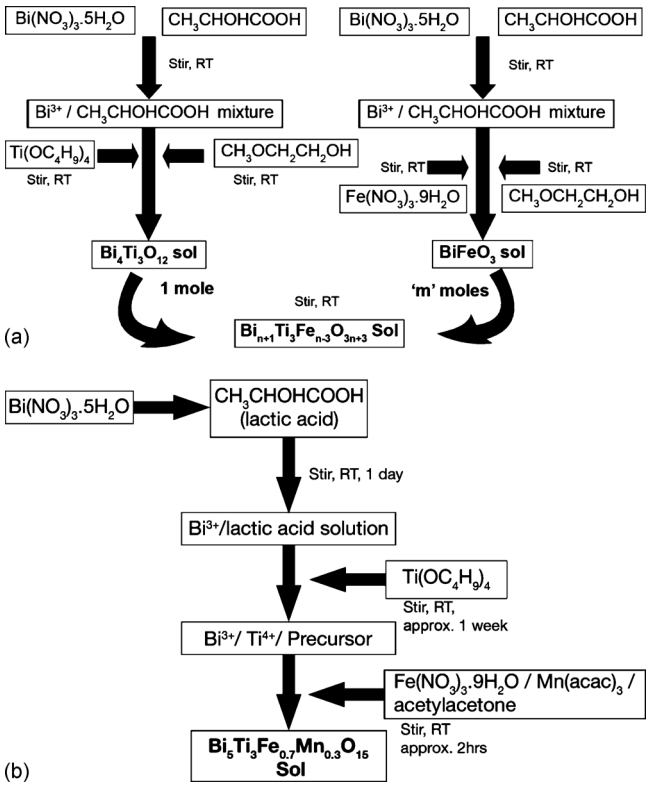

FIG. 1. Flow chart for the preparation of (a) $Bi_{n+1}Ti_3Fe_{n-3}O_{3n+3}$ and (b) $Bi_5Ti_3Fe_{0.7}Mn_{0.3}O_{15}$ sols.

a)Electronic mail: lynette.keeney@tyndall.ie.

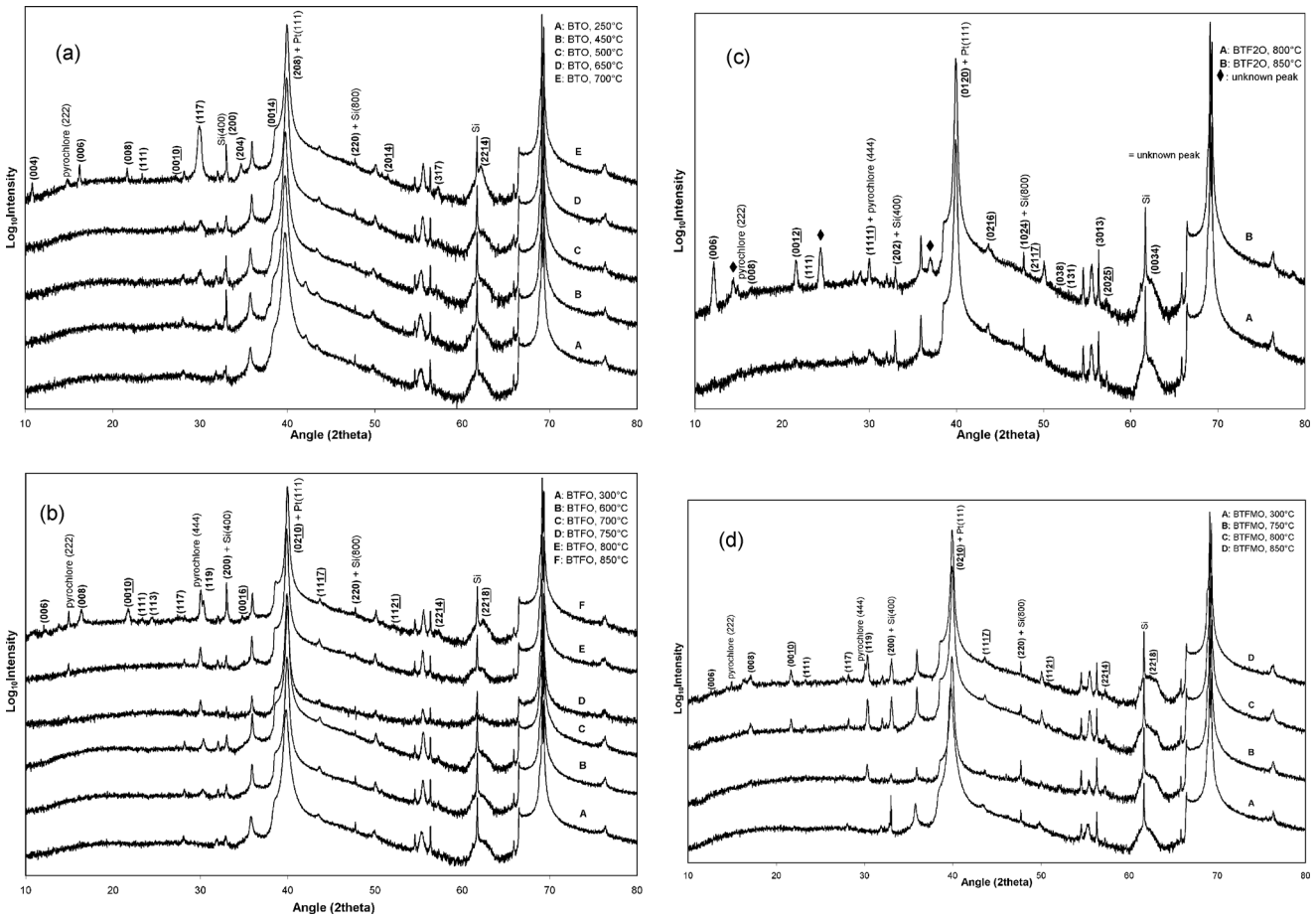

FIG. 2. XRD patterns of (a) $Bi_4Ti_3O_{12}$, (b) $Bi_5Ti_3FeO_{15}$, (c) $Bi_6Ti_3Fe_2O_{18}$, and (d) $Bi_5Ti_3Fe_{0.7}Mn_{0.3}O_{15}$ thin films annealed at various temperatures.

tric effect around room temperature) by substituting Mn^{3+} ions for Fe^{3+} ions in $BiFeO_3$. At a Néel temperature of 420 K for $BiFe_{0.7}Mn_{0.3}O_3$, positive magnetocapacitance effects were demonstrated at room temperature (0.3% magnetocapacitance effect at 9 T).

Piezoreponse force microscopy (PFM) has emerged as a powerful technique for probing nanoscale phenomena in piezoelectric and ferroelectric materials on the nanometer and micrometer scales.[25–34] PFM is based on the detection of a bias-induced piezoelectric surface deformation.[35] A conductive tip is brought into contact with a piezoelectric sample surface, and the tip deflection resulting from the expansion or contraction of the sample due to the applied bias is measured. Both the magnitude and sign of the displacement can be translated into images of local piezoresponse and polarization direction. PFM spectroscopy modes can locally generate hysteresis loops and thereby provide information on local ferroelectric behavior in ferroelectric materials.[36–38]

In this study, sol-gel preparation of $Bi_4Ti_3O_{12}$ ($n=3$), $Bi_5Ti_3FeO_{15}$ ($n=4$), $Bi_6Ti_3Fe_2O_{18}$ ($n=5$), and $Bi_5Ti_3Fe_{0.7}Mn_{0.3}O_{15}$ ($n=4$) and deposition of thin films on $Pt/Ti/SiO_2-Si$ substrates are reported. A preparation where 30% of the Fe^{3+} ions in $Bi_5FeTi_3O_{15}$ are substituted with Mn^{3+} ions to form thin films of $Bi_5Ti_3Fe_{0.7}Mn_{0.3}O_{15}$ is described for the first time. The local electromechanical activity of these materials was investigated by PFM.

II. EXPERIMENTAL

$Bi_4Ti_3O_{12}$ (BTO) sols were prepared from bismuth nitrate pentahydrate $[Bi(NO_3)_3\cdot 5H_2O]$ and tetra-*n*-butyl titanate $[Ti(OC_4H_9)_4]$ in a similar manner to the room temperature procedure described by Du *et al.*[39] On addition of 2-methoxyethanol ($CH_3OCH_2CH_2OH$), the viscosity and surface tension of the sols could be adjusted and 0.2 mol dm^{-3} sols were obtained.

Sols of $BiFeO_3$ were prepared by adding the required amounts of $Bi(NO_3)_3\cdot 5H_2O$ and iron(III) nitrate nonahydrate $[Fe(NO_3)_3\cdot 9H_2O]$ to a lactic acid ($CH_3CHOHCOOH$)/2-methoxyethanol mixture. The sols were stirred at room temperature until complete dissolution was achieved. On combination of $Bi_4Ti_3O_{12}$ with "*m*" moles of $BiFeO_3$, where $m=1$ and 2, 0.1 mol dm^{-3} sols of $Bi_5Ti_3FeO_{15}$ (BTFO) and $Bi_6Ti_3Fe_2O_{18}$ (BTF2O), respectively, were attained, as illustrated in the flow chart in Fig. 1(a).

For the preparation of $Bi_5Ti_3Fe_{0.7}Mn_{0.3}O_{15}$ [Fig. 1(b)], the required amounts of $Bi(NO_3)_3\cdot 5H_2O$ and $Ti(OC_4H_9)_4$ were dissolved in lactic acid at room temperature. $Fe(NO_3)_3\cdot 9H_2O$ and $Mn(C_5H_7O_2)_3$ [manganese(III) acetylacetonate] were dissolved separately in acetylacteone. When complete dissolution was achieved, this solution was slowly dropped into the Bi^{3+}/Ti^{4+} solution under constant stirring to

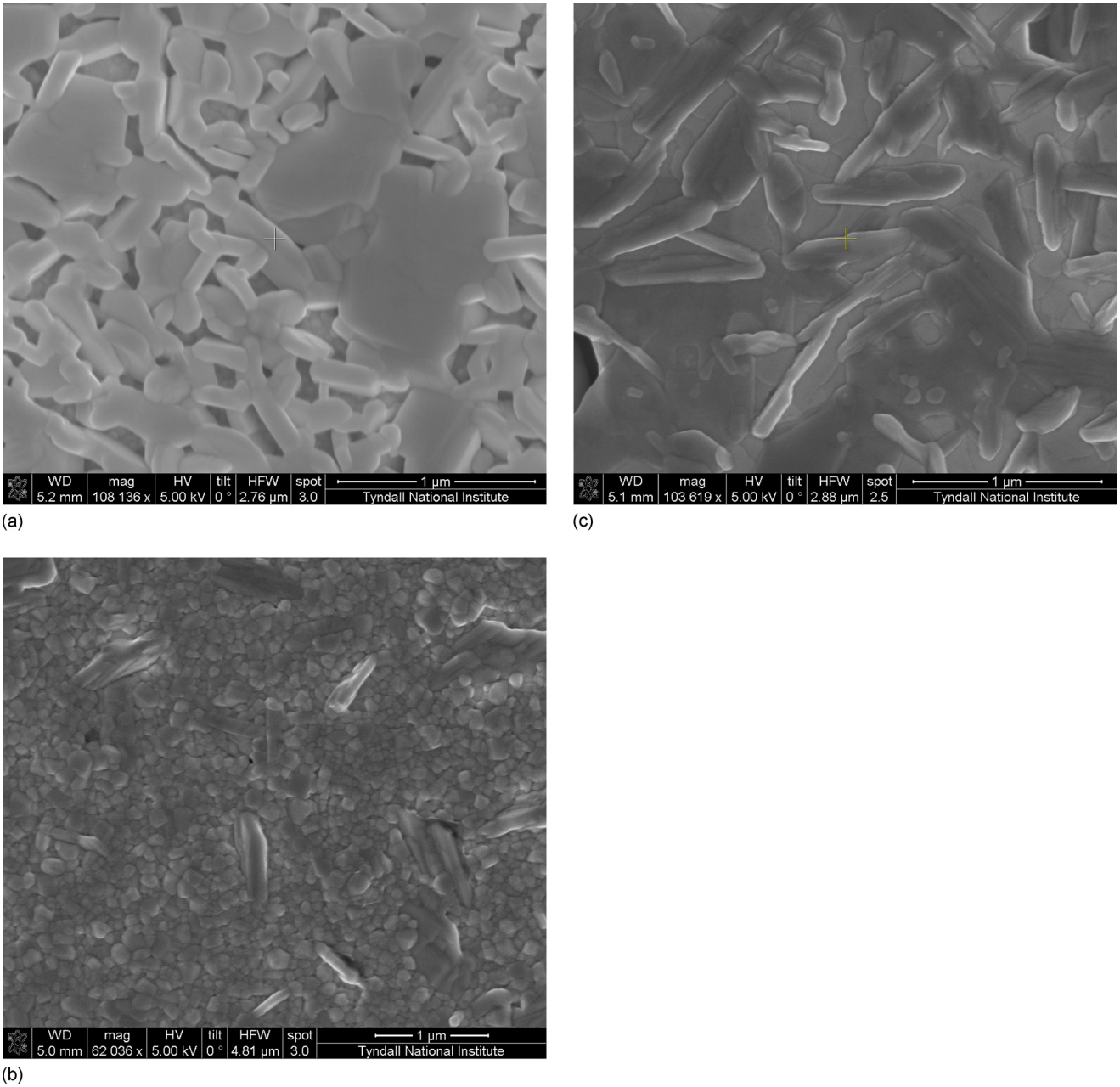

FIG. 3. (Color online) HRSEM images of (a) BTO annealed at 700 °C, (b) BTFO annealed at 850 °C, and (c) BTF2O annealed at 850 °C.

prepare 0.13 mol dm^{-3} sols of $Bi_5Ti_3Fe_{0.7}Mn_{0.3}O_{15}$ (BTFMO).

For all sols, a minimum of 5.0 mol % excess Bi was used to compensate evaporation of bismuth during the annealing process. Investigations have shown that addition of at least 5.0 mol % excess Bi to the sols suppresses the formation of pyrochlore phase $Bi_2Ti_2O_7$ in $Bi_5Ti_3FeO_{15}$ thin films.[40] Prevention of the formation of pyrochlore phase has also been demonstrated in sol-gel PZT films with the addition of excess Pb to the sols.[41]

The films were spin coated on $Pt/Ti/SiO_2/Si$ substrates using a commercial spinner (spin coater KW-4A, Chemat Technology) operating at 4300 rpm (BTO, BTFO, and BTF2O) or 4500 rpm (BTFMO) for 30 s yielding films of thicknesses ranging from ~100 to ~250 nm, as observed in cross-section scanning electron microscope (SEM) measurements. Excess solvents and residual organics were removed from the films by baking on calibrated hot plate at 250.0 ± 5.0 °C (BTO) or 300.0 ± 5.0 °C (BTFO, BTF2O, and BTFMO) for approximately 10 min. The films were annealed in ambient air at various temperatures for 1 h in a conventional furnace.

X-ray diffraction (XRD) profiles were recorded at room temperature using a Phillips Xpert PW3719 MPD diffractometer, equipped with a Cu $K\alpha$ radiation source (40 kV and 35 mA) over the range $10° \leq 2\theta \leq 80°$.

Topography was examined using scanning electron microscopy and atomic force microscopy. SEM images were obtained from the electron microscopy and analysis facility, Tyndall National Institute, using a FEI Nova 630 high resolution SEM (HRSEM). A commercial atomic force microscope (AFM) (MFP-3D™, Asylum Research) in ac mode was used for topography mapping of the films. Olympus

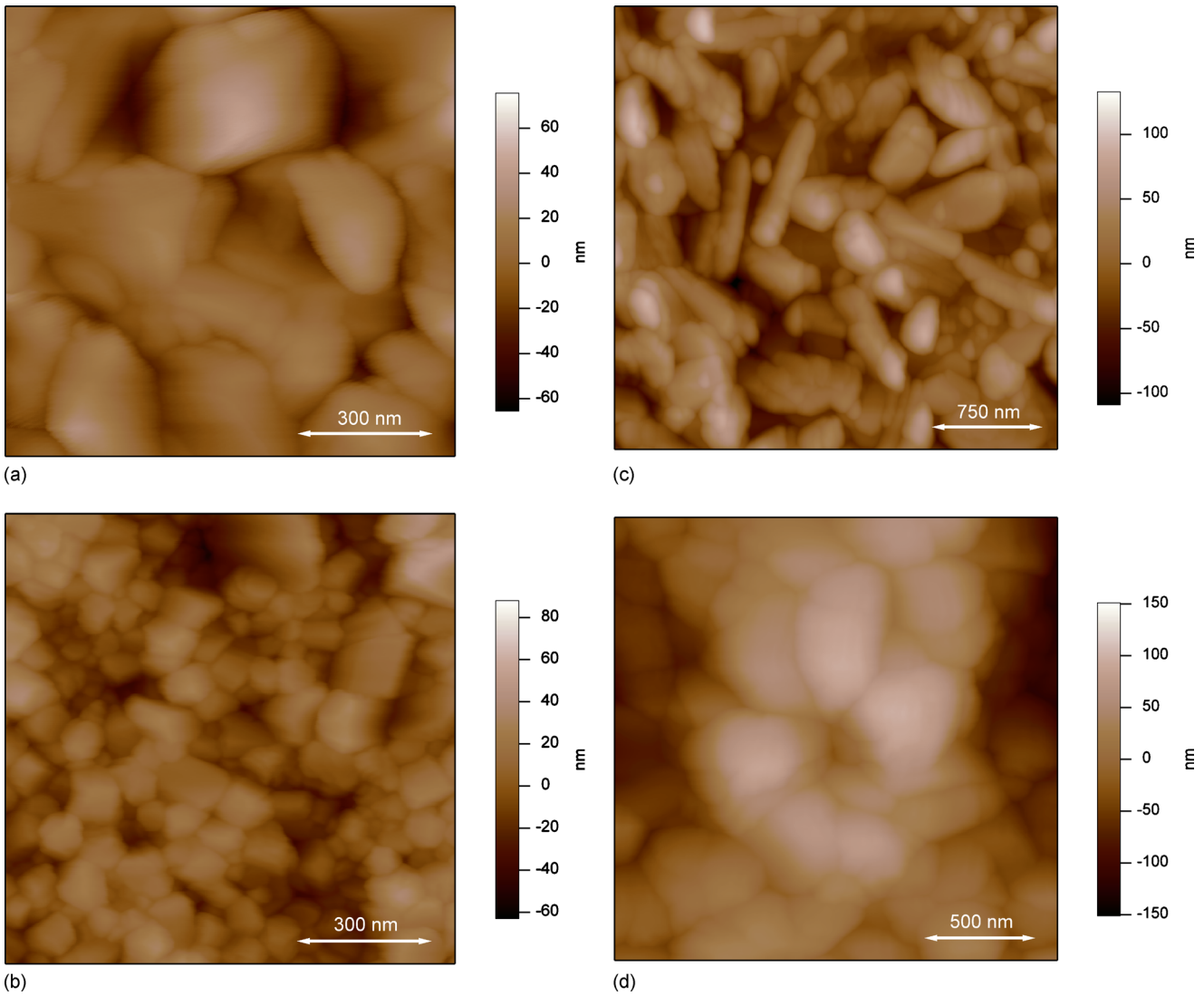

FIG. 4. (Color online) AFM images of (a) BTO annealed at 700 °C (rms roughness=16.5 nm), (b) BTFO annealed at 850 °C (rms roughness ranged from 15.1 to 67.6 nm), (c) BTF2O annealed at 850 °C (rms roughness=29.3 nm), and (d) BTFMO annealed at 800 °C (rms roughness=35.4 nm).

AC240TS silicon cantilevers (Al reflex coated, 70 kHz resonant frequency) were used for imaging.

Electromechanical responses of the films were investigated by dual frequency resonance tracking PFM (DFRT-PFM) using an Asylum Research MFP-3D™ AFM in contact mode equipped with a HVA220 Amplifier for PFM. Imaging with the DFRT-PFM technique allows an enhanced electromechanical response by operation of the cantilever near resonance, while reducing crosstalk between changes in the contact stiffness and the PFM signal by tracking the resonance frequency based on amplitude detection feedback.[42] Olympus AC240TM Electrilevers, Pt/Ir coated silicon cantilevers (Al reflex coated, 70 kHz resonant frequency, ~320 kHz contact resonance frequency) were used for vertical PFM imaging.

III. RESULTS AND DISCUSSION

A. Crystal structure

Figure 2(a) shows the XRD results of the BTO thin films annealed over the temperature range of 300–700 °C. The BTO films begin to crystallize at annealing temperatures of 500 °C, indicated by the presence of the (117) peak. As the annealing temperature increases, the peak becomes sharper and the full width at half maximum (FWHM) decreases (0.402° at 500 °C compared with 0.100° at 700 °C) indicating improved crystallinity and an increase in grain size with increasing annealing temperatures. For films annealed at 700 °C, orthorhombic $Bi_4Ti_3O_{12}$ [Joint Committee for Powder Diffraction Standard (JCPDS) No. 72-1019] is the predominant phase, with pronounced crystallization of $Bi_4Ti_3O_{12}$ grains as indicated by the relatively sharp diffraction patterns. Strong reflections of the (117), (006), and (008) planes are evident, associated with a layered perovskite structure. However, a minor impurity peak at $2\theta=15°$ may be considered to be bismuth-based pyrochlore phases including $Bi_2Ti_2O_7$ (JCPDS No. 32-0118). Given that the intensity of the (117) peak is dominant with respect to the (00*l*) peaks; the $Bi_4Ti_3O_{12}$ phase appears to be randomly oriented.[43] Lack of *c*-axis orientation has been observed previously for $Bi_4Ti_3O_{12}$ films deposited on $Pt/Ti/SiO_2/Si$ substrates.[44]

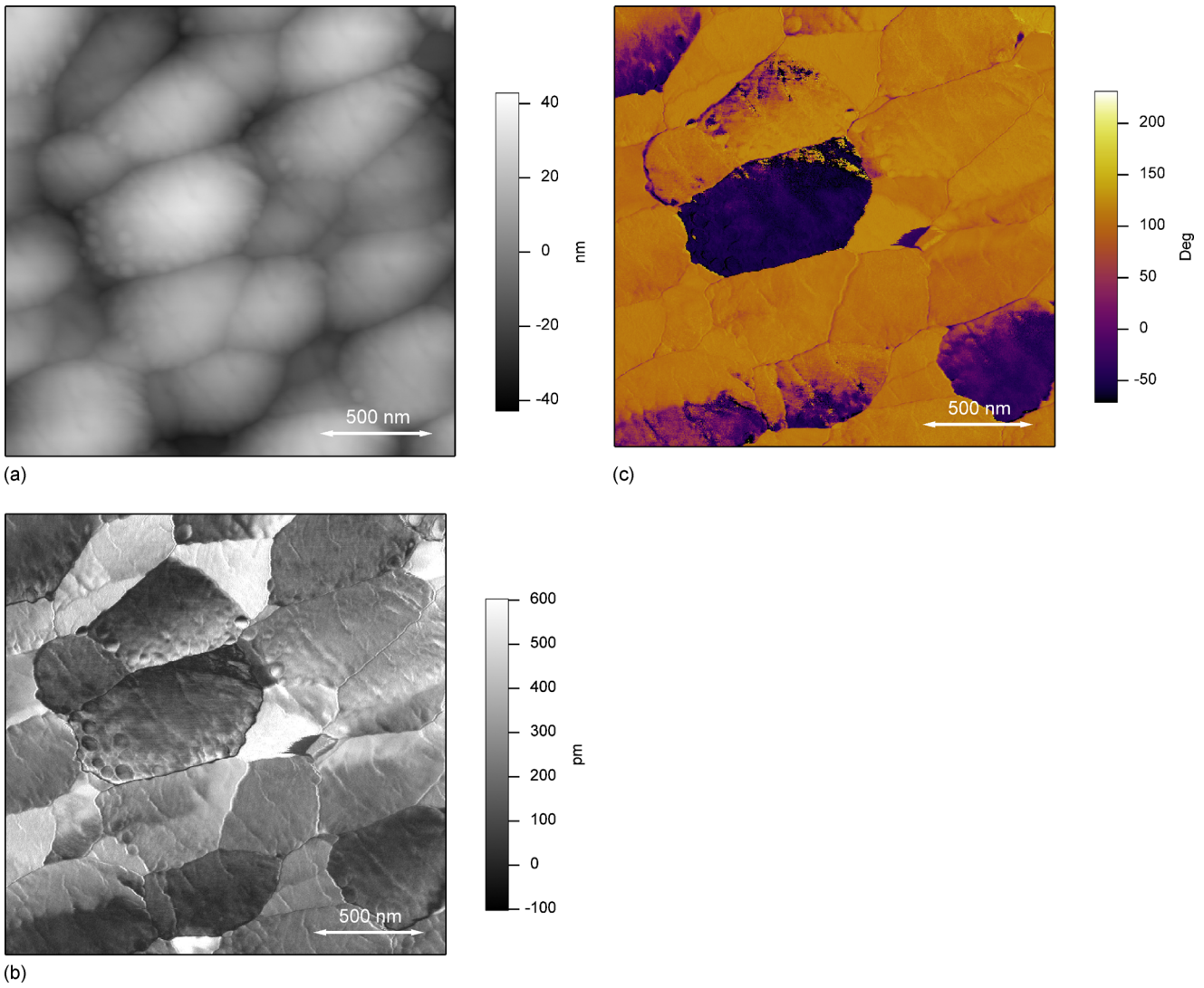

FIG. 5. (Color online) (a) Topography, (b) piezoresponse amplitude, and (c) piezoresponse phase images of BTO annealed at 700 °C.

The XRD patterns of BTFO films annealed over the temperature range of 300–850 °C are shown in Fig. 2(b). The results demonstrate that the films of the layered perovskite phase of $Bi_5Ti_3FeO_{15}$ were successfully obtained at 850 °C (JCPDS No. 38-1257); however, the pyrochlore phase of $Bi_2Ti_2O_7$ also existed. Formation of the (119) peak begins at annealing temperature of 600 °C and the intensity of the peak increases with increasing annealing temperatures, however the peak splits into two subpeaks at 850 °C, revealing the presence of the (444) reflection of pyrochlore $Bi_2Ti_2O_7$. The results demonstrate that annealing above 750 °C gives rise to pyrochlore (222) impurity peaks, while annealing below 850 °C leads to incomplete crystallization of the $Bi_5Ti_3FeO_{15}$ phase.

Figure 2(c) illustrates the XRD results of the BTF2O thin films annealed over the temperature range of 800–850 °C. The results demonstrate the presence of layered Aurivillius phase $Bi_6Ti_3Fe_2O_{18}$ (JCPDS No. 21-0101) at 850 °C, however $Bi_2Ti_2O_7$ pyrochlore and unknown impurity phases at 2θ=14.4°, 24.5°, and 37.1° also existed. The unknown peaks could be attributed to the presence of $Bi_2Fe_4O_9$ (JCPDS No. 74-1098). However, further work is needed to investigate the formation of impurities and control the crystallinity of the $Bi_6Ti_3Fe_2O_{18}$ films. Energy dispersive x-ray analysis spectra confirmed that iron was successfully inserted into the Aurivillius structures of $Bi_5Ti_3FeO_{15}$ and $Bi_6Ti_3Fe_2O_{18}$.

The XRD patterns of BTFMO films annealed over the temperature range of 300–850 °C are displayed in Fig. 2(d). Crystallization of the BTFMO films begins at annealing temperatures of 750 °C, denoted by the presence of the (119) peak (FWHM=0.117). The intensity of this peak increased (FWHM=0.100) and the XRD pattern of BTFMO at 800 °C coincided well with that of $Bi_5Ti_3FeO_{15}$ as reported in the literature (JCPDS No. 38-1257),[45] indicating that the orthorhombic phase is preserved with 30% Mn^{3+} substitution. This observation is consistent with previous powder XRD studies on $Bi_5Ti_3Fe_{0.7}Mn_{0.3}O_{15}$ ceramics.[9] The incorporation of Mn^{3+} in the place of Fe^{3+} has reduced the crystallization temperature of BTFMO compared to that of BTFO. Pyrochlore $Bi_2Ti_2O_7$ phases are noted for BTFMO annealed at 850 °C and a further impurity peak is observed at 2θ =16.6°, possibly due to the presence of Mn_2O_3 (JCPDS No. 38-1257) or other metal oxide impurities.

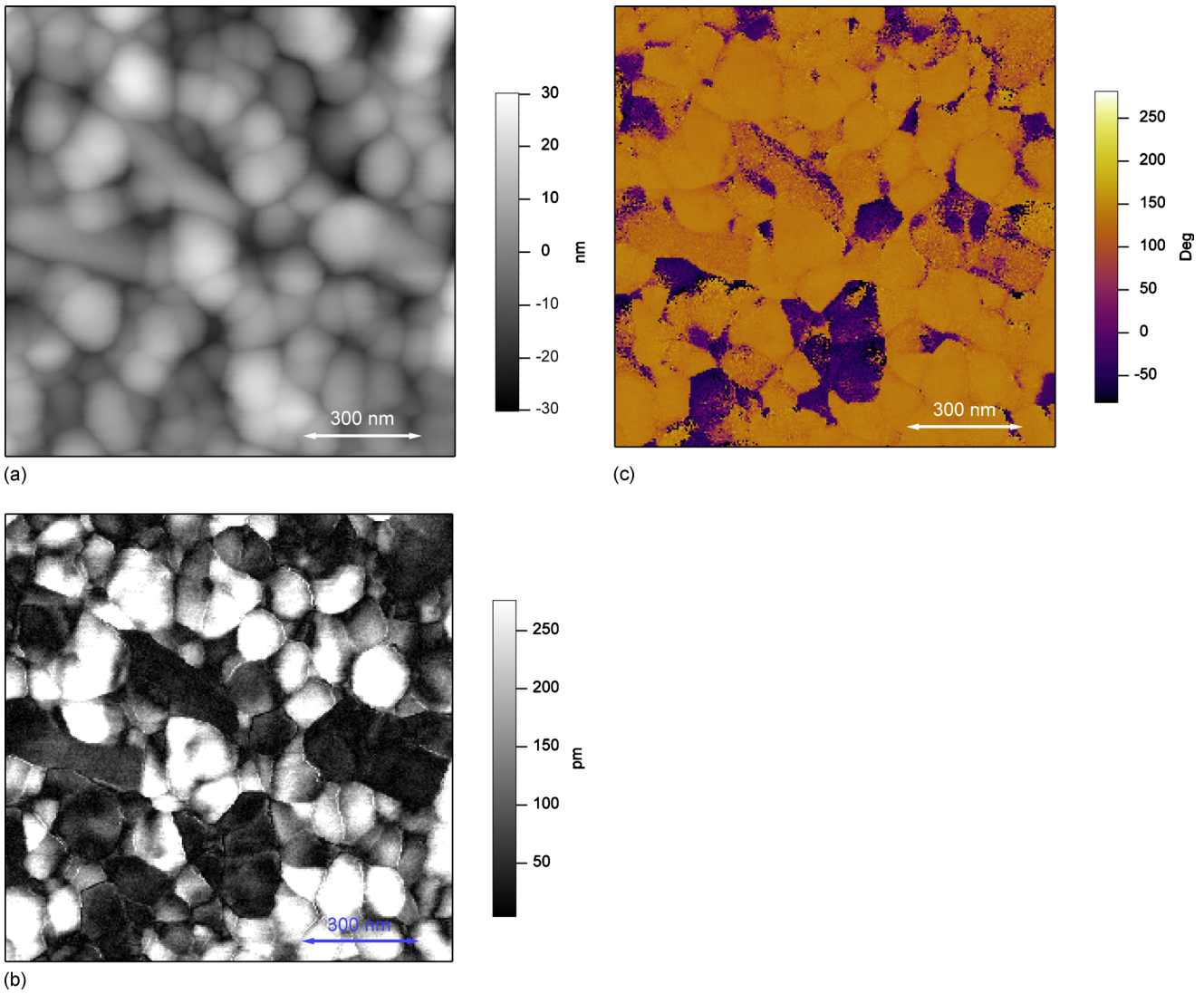

FIG. 6. (Color online) (a) Topography, (b) piezoresponse amplitude, and (c) piezoresponse phase images of BTFO annealed at 850 °C.

B. Surface morphology

The films were characterized by a dense, crack-free microstructure as demonstrated by HRSEM and AFM techniques which were used to examine the surface morphology of the films. Representative HRSEM images displayed in Fig. 3 reveal layered phases crystallized in platelike morphologies. Such morphology is characteristic of layer structures of the Aurivillius type.[46] The SEM image of BTO annealed at 700 °C reveal lamellar grains of different orientation overlapping one another. The SEM micrograph of BTFO annealed at 850 °C shows the formation of aggregates of smaller particles, along with unevenly distributed discrete platelike grains. The BTF2O sample annealed at 850 °C exhibits an increase in particle size with a large number of distinct platelets throughout the surface.

Typical AFM images of the thin films and the corresponding root mean square (rms) roughness values are displayed in Fig. 4. The average grain size was estimated to be 390 nm, 730 nm, and 490 nm for BTO (800 °C), BTF2O (850 °C), and BTFMO (800 °C), respectively. The grain size and roughness of the BTFO film annealed at 850 °C ranged from approximately 180 nm to 1.2 μm over different regions analyzed on the film, in accordance with the observation of unevenly distributed plate-like grains in the HRSEM micrographs of the sample. Average grain size and rms roughness values generally increased with increased annealing temperature, in accordance with the XRD pattern results where improved crystallinity and decreased FWHM values were achieved with increasing annealing temperatures. The exception was for the BTFMO samples, where rms roughness values increased from 0.509 nm and 24.4 nm for the samples annealed at 300 °C and 700 °C, respectively, and to 35.4 nm for the sample annealed at 800 °C. However, the rms roughness decreased to 20.8 nm for the sample annealed at 850 °C. The reasons for this apparent anomaly are as yet unclear, although it is possible that impurity phases present in the sample annealed at 850 °C [as evident in XRD pattern Fig. 2(d)] may have an effect on the surface morphology of the films. For instance, Bi_2O_3 and Mn_2O_3 or other metal oxide impurities may evolve at the higher temperature and form a eutectic composition[47] on the surface of the film. This discrepancy could also arise from

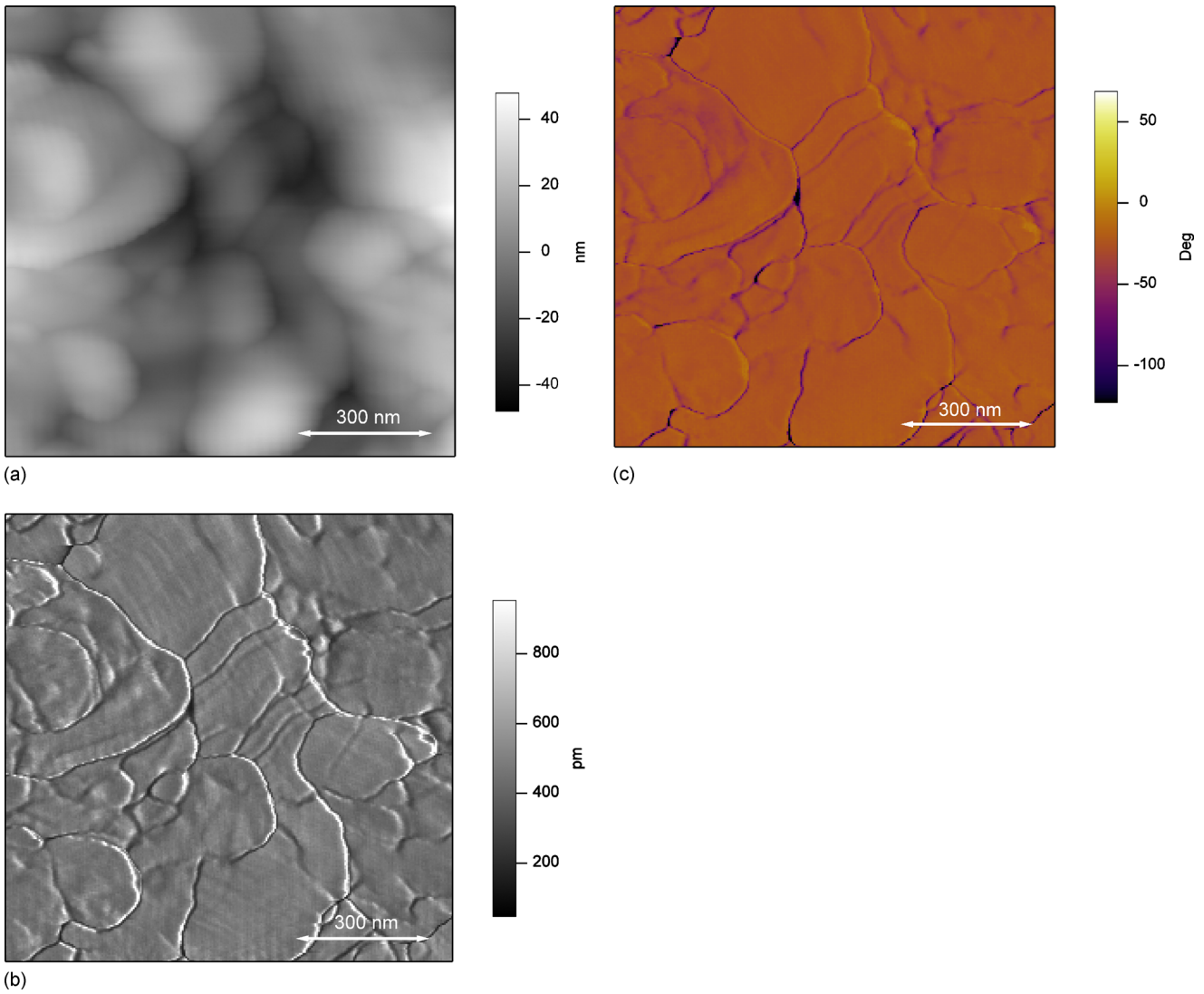

FIG. 7. (Color online) (a) Topography, (b) piezoresponse amplitude, and (c) piezoresponse phase images of BTF2O annealed at 850 °C.

thermal mismatches of the sub lattices in the sample annealed at the higher temperature.

C. Piezoelectric properties

Characteristic vertical PFM images of BTO (700 °C), BTFO (850 °C), BTF2O (850 °C), and BTFMO (800 °C) are shown in Figs. 5–8, respectively.

The phase of the local electromechanical response of the surface provides information on the polarization orientation of the sample when an oscillating voltage is applied to the sample with a conductive tip of the AFM. The response amplitude provides a measure of the local electromechanical activity of the surface. In the piezoelectric images, domains with opposite polarities exhibit different phase contrast. Negative domains correspond to domains with polarization oriented toward the substrate (φ=180°), and positive domains corresponded to domains with polarization terminated at the free surface of the film (φ=0°). Since the vertical PFM technique is sensitive only to the component of polarization normal to the film surface, grains with in-plane polarization (with vanishing out-of-plane polarization) will exhibit an intermediate contrast.[48]

The results indicate that the BTO, BTFO, and BTFMO samples analyzed have piezoelectric properties. The average response of the negatively polarized domains differs to that of the positive ones in the BTO, BTFO, and BTMO thin films, indicating that these films are naturally self-polarized. In the BTO and BTFO films, mainly single domain grains were observed. For the BTMO films, grains tend to be mostly single domain with some multi-domain character.

Vertical PFM images of BTF2O illustrate relatively weak amplitude contrast and minor (~25°) phase variations within the film. The lack of appreciable electromechanical response is indicative of a BTF2O film rich in pyrochlore phase or other nonpiezoelectric impurity phases. The slight response observed is likely due to surface deformation generated by tip-surface electrostatic forces, rather than inherent electromechanical coupling in the material. Alternatively, the film could be comprised of domains with the polarization vector within the film plane or domains with the polarization vector deviating from the direction normal to the film plane.

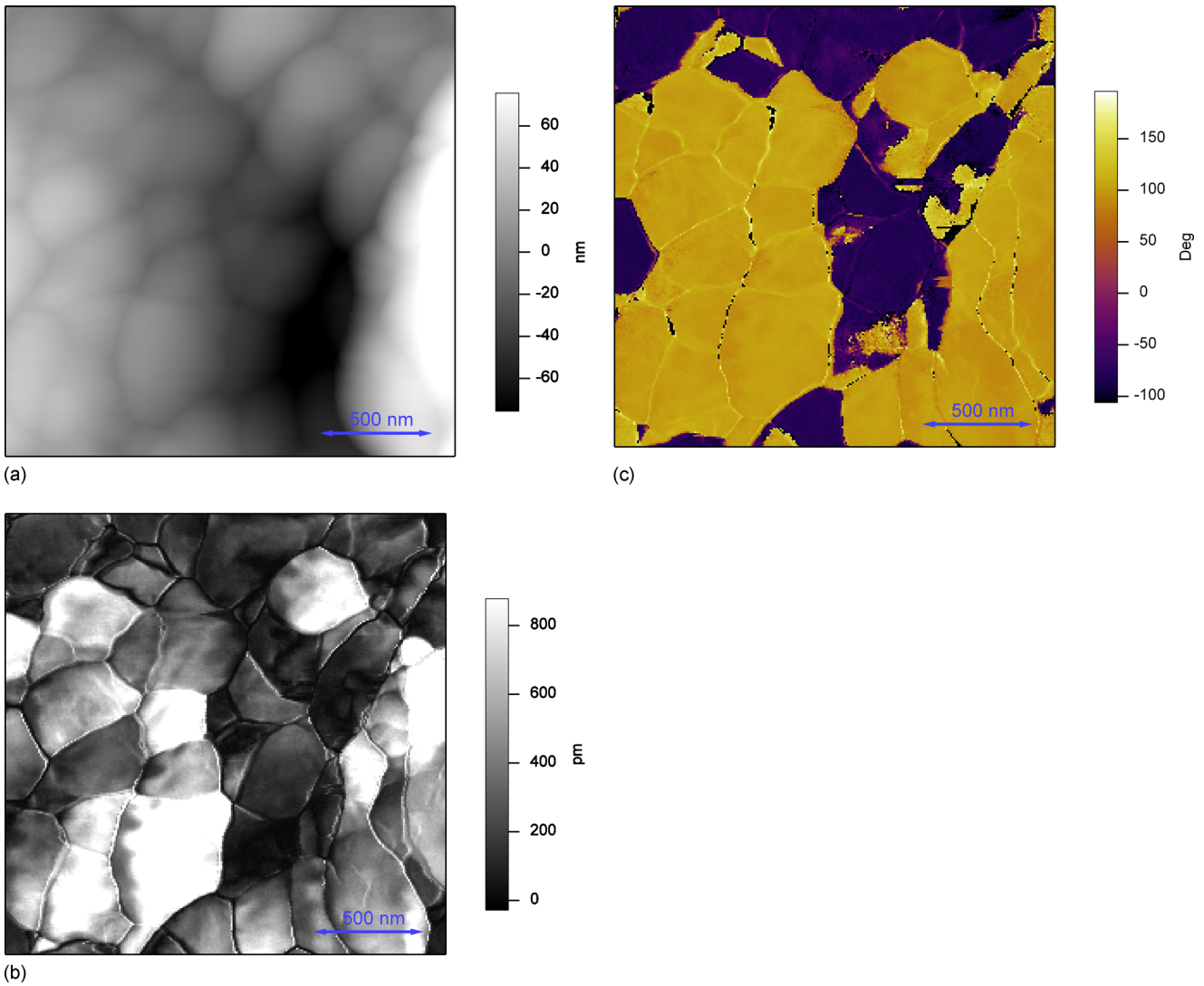

FIG. 8. (Color online) (a) Topography, (b) piezoresponse amplitude, and (c) piezoresponse phase images of BTFMO annealed at 800 °C.

The vertical piezoelectric signal from these domains should be weaker than from vertical-domains.[25] Lateral PFM imaging would provide information on any in-plane components of polarization in the samples.

IV. CONCLUSIONS

Thin films of Aurivillius phase $Bi_4Ti_3O_{12}$ ($n=3$), $Bi_5Ti_3FeO_{15}$ ($n=4$), $Bi_6Ti_3Fe_2O_{18}$ ($n=5$), and $Bi_5Ti_3Fe_{0.7}Mn_{0.3}O_{15}$ ($n=4$) deposited on $Pt/Ti/SiO_2-Si$ substrates were synthesized by sol-gel methods and a preparation for $Bi_5Ti_3Fe_{0.7}Mn_{0.3}O_{15}$ thin films is described for the first time. XRD data demonstrated that the Aurivillius phase materials were successfully obtained, however pyrochlore phases of $Bi_2Ti_2O_7$ were present in some cases. Higher annealing temperatures than those used for BTO thin films were required for crystallization of the $n \geq 4$ phase materials. HRSEM and AFM analysis of the films revealed microstructure characteristic of Aurivillius phase layer structures. Local electromechanical responses of the films were investigated by DFRT-PFM where the $Bi_4Ti_3O_{12}$, $Bi_5Ti_3FeO_{15}$, and $Bi_5Ti_3Fe_{0.7}Mn_{0.3}O_{15}$ films demonstrated piezoelectric properties, however no significant piezoelectric response was observed for $Bi_6Ti_3Fe_2O_{18}$ samples in the vertical PFM mode. Given the coexistence of pyrochlore phase of $Bi_2Ti_2O_7$ in the $Bi_4Ti_3O_{12}$, $Bi_5Ti_3FeO_{15}$, and $Bi_6Ti_3Fe_2O_{18}$ films analyzed in this study by PFM, it is expected that single-phase films would have enhanced piezoelectric properties.

ACKNOWLEDGMENTS

The support of Science Foundation Ireland (SFI) under the FORME Strategic Research Cluster Award No. 07/SRC/I1172 and the European Union under the CAMELIA Specific Targeted Research or Innovation Project Contract No. STRP 033103 is gratefully acknowledged.

[1]L. W. Martin, S. P. Crane, Y. H. Chu, M. B. Holcomb, M. Gajek, M. Huijben, C. H. Yang, N. Balke, and R. Ramesh, J. Phys.: Condens. Matter **20**, 434220 (2008).
[2]B. Aurivillius, Ark. Kemi **1**, 499 (1949).
[3]S. B. Desu, P. C. Joshi, X. Zhang, and S. O. Ryu, Appl. Phys. Lett. **71**, 1041 (1997).
[4]M. D. Maeder, D. Damjanovic, and N. Setter, *Lead Free Piezoelectric Materials* (Kluwer Academic, Cambridge, MA, 2003), pp. 385–392.
[5]J. F. Scott, Jpn. J. Appl. Phys., Part 1 **38**, 2272 (1999).
[6]S. Y. Wu, W. J. Takei, and M. H. Francombe, Ferroelectrics **10**, 209 (1976).

[7]S. Patri, R. Choudhary, and B. Samantaray, J. Electroceram. **20**, 119 (2008).
[8]H. Irie, M. Miyayama, and T. Kudo, J. Appl. Phys. **90**, 4089 (2001).
[9]S.-l. Ahn, Y. Noguchi, M. Miyayama, and T. Kudo, Mater. Res. Bull. **35**, 825 (2000).
[10]A. Z. Simões, M. A. Ramirez, C. S. Riccardi, E. Longo, and J. A. Varela, Mater. Lett. **60**, 2020 (2006).
[11]A. Z. Simões, M. A. Ramirez, A. Ries, J. A. Varela, E. Longo, and R. Ramesh, Appl. Phys. Lett. **88**, 072916 (2006).
[12]A. Z. Simoes, C. S. Riccardi, A. Ries, M. A. Ramirez, E. Longo, and J. A. Varela, J. Mater. Process. Technol. **196**, 10 (2008).
[13]S. Patri and R. Choudhary, Appl. Phys. A: Mater. Sci. Process. **94**, 321 (2009).
[14]A. Sanson and R. W. Whatmore, Jpn. J. Appl. Phys., Part 1 **41**, 7127 (2002).
[15]A. Sanson and R. W. Whatmore, J. Am. Ceram. Soc. **88**, 3147 (2005).
[16]H. Zhang, H. Yan, and M. J. Reece, J. Appl. Phys. **106**, 044106 (2009).
[17]X. Mao, W. Wang, X. Chen, and Y. Lu, Appl. Phys. Lett. **95**, 082901 (2009).
[18]H.-X. Lu, X.-Y. Mao, W. Wang, and X.-B. Chen, PIERS Proceedings, Hangzhou, China, March 24-28,2008, pp. 1093–1096.
[19]Y. Noguchi, K. Yamamoto, Y. Kitanaka, and M. Miyayama, J. Eur. Ceram. Soc. **27**, 4081 (2007).
[20]C. H. Yang, T. Y. Koo, and Y. H. Jeong, Solid State Commun. **134**, 299 (2005).
[21]M. M. Kumar, A. Srinivas, G. S. Kumar, and S. V. Suryanarayana, Solid State Commun. **104**, 741 (1997).
[22]T. Kimura, S. Kawamoto, I. Yamada, M. Azuma, M. Takano, and Y. Tokura, Phys. Rev. B **67**, 180401 (2003).
[23]V. R. Palkar, J. John, and R. Pinto, Appl. Phys. Lett. **80**, 1628 (2002).
[24]J. B. Goodenough, Phys. Rev. **100**, 564 (1955).
[25]A. Gruverman, O. Auciello, R. Ramesh, and H. Tokumoto, Nanotechnology **8**, A38 (1997).
[26]S. V. Kalinin, B. J. Rodriguez, S. Jesse, E. Karapetian, B. Mirman, E. A. Eliseev, and A. N. Morozovska, Annu. Rev. Mater. Res. **37**, 189 (2007).
[27]N. Balke, I. Bdikin, S. V. Kalinin, and A. L. Kholkin, J. Am. Ceram. Soc. **92**, 1629 (2009).
[28]D. A. Bonnell, S. V. Kalinin, A. L. Kholkin, and A. Gruverman, MRS Bull. **34**, 648 (2009).
[29]J. Guyonnet, H. Bea, F. Guy, S. Gariglio, S. Fusil, K. Bouzehouane, J. M. Triscone, and P. Paruch, Appl. Phys. Lett. **95**, 132902 (2009).
[30]M. J. Lowe, T. Hegarty, K. Mingard, J. Li, and M. G. Cain, Integr. Ferroelectr. **98**, 136 (2008).
[31]L. McGilly, D. Byrne, C. Harnagea, A. Schilling, and J. M. Gregg, J. Mater. Sci. **44**, 5197 (2009).
[32]F. Peter, A. Rudiger, R. Dittmann, R. Waser, K. Szot, B. Reichenberg, and K. Prume, Appl. Phys. Lett. **87**, 082901 (2005).
[33]F. Johann, T. Jungk, S. Lisinski, A. Hoffmann, L. Ratke, and E. Soergel, Appl. Phys. Lett. **95**, 202901 (2009).
[34]B. J. Rodriguez, X. S. Gao, L. F. Liu, W. Lee, I. I. Naumov, A. M. Bratkovsky, D. Hesse, and M. Alexe, Nano Lett. **9**, 1127 (2009).
[35]S. V. Kalinin, B. J. Rodriguez, S. Jesse, P. Maksymovych, K. Seal, M. Nikiforov, A. P. Baddorf, A. L. Kholkin, and R. Proksch, Mater. Today **11**, 16 (2008).
[36]S. Jesse, A. P. Baddorf, and S. V. Kalinin, Appl. Phys. Lett. **88**, 062908 (2006).
[37]S. V. Kalinin, A. Gruverman, and D. A. Bonnell, Appl. Phys. Lett. **85**, 795 (2004).
[38]S. Jesse, H. N. Lee, and S. V. Kalinin, Rev. Sci. Instrum. **77**, 073702 (2006).
[39]X. Du, Y. Xu, H. Ma, J. Wang, and X. Li, J. Am. Ceram. Soc. **91**, 2079 (2008).
[40]L. Keeney, C. Groh, M. E. Pemble, and R. W. Whatmore (unpublished).
[41]J. M. Marshall, Q. Zhang, Z. Huang, and R. W. Whatmore, Ferroelectrics **318**, 41 (2005).
[42]B. J. Rodriguez, C. Callahan, S. V. Kalinin, and R. Proksch, Nanotechnology **18**, 475504 (2007).
[43]P. Fuierer and B. Li, J. Am. Ceram. Soc. **85**, 299 (2002).
[44]H. Wang, Mater. Sci. Eng., B **111**, 64 (2004).
[45]F. Kubel and H. Schmid, Ferroelectrics **129**, 101 (1992).
[46]J. Rymarczyk, A. Hanc, G. Dercz, and J. Ilczuk, Acta Phys. Pol. A **114**, 1579 (2008).
[47]Y. F. Kargin and V. Y. Voevodskii, Russ. J. Inorg. Chem. **45**, 1412 (2000).
[48]A. Wu, P. M. Vilarinho, V. V. Shvartsman, G. Suchaneck, and A. L. Kholkin, Nanotechnology **16**, 2587 (2005).